

# Graviton production through photon-quark scattering at the LHC

İ. Şahin,<sup>1,\*</sup> M. Köksal,<sup>2,†</sup> S. C. İnan,<sup>2,‡</sup> A. A. Billur,<sup>2,§</sup>

B. Şahin,<sup>1,¶</sup> P. Tektaş,<sup>1</sup> E. Alıcı,<sup>3</sup> and R. Yıldırım<sup>2</sup>

<sup>1</sup>*Department of Physics, Faculty of Sciences,  
Ankara University, 06100 Tandogan, Ankara, Turkey*

<sup>2</sup>*Department of Physics, Cumhuriyet University, 58140 Sivas, Turkey*

<sup>3</sup>*Department of Physics, Bulent Ecevit University, 67100 Zonguldak, Turkey*

## Abstract

We have investigated real graviton emission in the ADD and RS model of extra dimensions through the photoproduction process  $pp \rightarrow p\gamma p \rightarrow pGqX$  at the LHC. We have considered all contributions from the subprocesses  $\gamma q \rightarrow Gq$ , where  $q = u, d, c, s, b, \bar{u}, \bar{d}, \bar{c}, \bar{s}, \bar{b}$  quark. The constraints on model parameters of the ADD and RS model of extra dimensions have been calculated.

---

\*inancsahin@ankara.edu.tr

†mkoksal@cumhuriyet.edu.tr

‡sceminan@cumhuriyet.edu.tr

§abillur@cumhuriyet.edu.tr

¶banusahin@ankara.edu.tr

## I. INTRODUCTION

One of the leading aims of the Large Hadron Collider (LHC) is to discover new physics beyond the Standard Model. In this respect, extra dimensional models in particle physics have been drawing attention for the past fifteen years. These models offer a solution to the hierarchy problem, and provide possible candidates for dark matter. Phenomenology of extra dimensional models at the LHC has been widely studied in the literature as a possible new physics candidate. These phenomenological studies generally involve usual proton-proton deep inelastic scattering (DIS) processes where both of the colliding protons dissociate into partons. Subprocesses of quark-quark, gluon-gluon, and quark-gluon scattering have been probed in detail. On the other hand, exclusive production and semi-elastic processes have been much less studied in the literature. In an exclusive production process both of the incoming protons remains intact. They do not dissociate into partons. However in a semi-elastic scattering process, one of the incoming proton dissociate into partons but the other proton remains intact [1, 2]. The exclusive and semi-elastic proton processes are characterized by the interchange of photons or pomerons. The former generally give larger cross sections since the survival probability for processes involving a photon interchange is larger than that for a pomeron interchange. The exclusive and semi-elastic photon-mediated processes are sometimes called two-photon and photoproduction processes respectively. Phenomenology of extra dimensions has not been studied comprehensively in these types of processes. Extra dimensional models have been examined via the following two-photon processes:  $pp \rightarrow p\gamma\gamma p \rightarrow p\ell\bar{\ell}p$  [3],  $pp \rightarrow p\gamma\gamma p \rightarrow p\gamma\gamma p$  [4, 5],  $pp \rightarrow p\gamma\gamma p \rightarrow p\Phi p$  [6],  $pp \rightarrow p\gamma\gamma p \rightarrow pt\bar{t}p$  [7] and  $pp \rightarrow p\gamma\gamma p \rightarrow pGp$  [8]. As far as we know, except for our recent paper [9] phenomenology of extra dimensional models has not been studied and model parameters have not been constrained in any photoproduction process at the LHC. In our recent paper we have analyzed the virtual effects of Kaluza-Klein (KK) gravitons in  $pp \rightarrow p\gamma p \rightarrow p\gamma qX$ . In this paper we will investigate real KK graviton emission through the photoproduction process  $pp \rightarrow p\gamma p \rightarrow pGqX$  (Fig.1).  $pp \rightarrow p\gamma p \rightarrow pGqX$  consists of the

following subprocesses:

$$\begin{aligned}
& \text{(i) } \gamma u \rightarrow Gu & \text{(vi) } \gamma \bar{u} \rightarrow G\bar{u} \\
& \text{(ii) } \gamma d \rightarrow Gd & \text{(vii) } \gamma \bar{d} \rightarrow G\bar{d} \\
& \text{(iii) } \gamma c \rightarrow Gc & \text{(viii) } \gamma \bar{c} \rightarrow G\bar{c} \\
& \text{(iv) } \gamma s \rightarrow Gs & \text{(ix) } \gamma \bar{s} \rightarrow G\bar{s} \\
& \text{(v) } \gamma b \rightarrow Gb & \text{(x) } \gamma \bar{b} \rightarrow G\bar{b}
\end{aligned} \tag{1}$$

Therefore, in order to obtain the cross section for the main process  $pp \rightarrow p\gamma p \rightarrow pGqX$  we have to consider all contributions coming from subprocesses in (1).

In a photoproduction process emitted photons from the proton ought to carry a small amount of virtuality. (Otherwise, proton dissociates after the emission.) Thus, the equivalent photon approximation (EPA) can be successfully applied to a photoproduction process. In EPA we employ the formalism of [10–12], and take account of the electromagnetic form factors of the proton. Hence, EPA formula that we have used is different from the pointlike electron or positron case.

Exclusive two-photon and photoproduction processes can be distinguished from fully inelastic processes by the virtue of the following experimental signatures: After the elastic emission of a photon, proton is scattered with a small angle and escapes detection from the central detectors. This causes a missing energy signature called *forward large-rapidity gap*, in the corresponding forward region of the central detector [1, 2, 13]. This technique was successfully used at the Fermilab Tevatron by the CDF Collaboration. Exclusive production of  $\ell\bar{\ell}$ ,  $\gamma\gamma$ ,  $jj$  and  $J/\psi$  were observed experimentally [14–18]. CMS Collaboration has also observed exclusive production of  $\ell\bar{\ell}$  and  $W^+W^-$  pairs using early LHC data at  $\sqrt{s}=7$  TeV [19–21]. Another experimental signature can be implemented by forward proton tagging. There are some proposals that aim to equip ATLAS and CMS central detectors with very forward detectors (VFD) which can detect intact scattered protons with a large pseudo-rapidity. Forward proton tagging in VFD supports forward large-rapidity gap signatures obtained from the central detectors. Operation of VFD in conjunction with central detectors with a precise timing, can efficiently reduce backgrounds from pile-up events [22, 23]. It is argued that pile-up background grows rapidly with luminosity and becomes important for high luminosity runs at the LHC.

Apart from extra dimensions other new physics scenarios have also been studied via two-photon and photoproduction processes at the LHC. Phenomenological studies involve new physics scenarios such as supersymmetry, unparticles, technicolor, magnetic monopoles and model independent analysis of anomalous interactions [24–54].

## II. EXTRA DIMENSIONAL MODELS AND CROSS SECTIONS

In this paper we will focus on two different extra dimensional models, namely, Arkani-Hamed, Dimopoulos and Dvali (ADD) model of large extra dimensions [55–57] and Randall and Sundrum (RS) model of warped extra dimensions [58].

In the ADD model of extra dimensions, mass difference between consecutive graviton excited states is given approximately by the formula [59, 60]:

$$\Delta m \approx \frac{M_D^{\frac{2+\delta}{\delta}}}{\bar{M}_{Pl}^{\frac{2}{\delta}}} \quad (2)$$

We see from this formula that mass splitting is quite narrow. For instance, if we choose  $M_D = 1$  TeV and  $\delta = 4$  then  $\Delta m \approx 50$  KeV. Therefore, at collider energies KK graviton production processes involve a summation over huge number of graviton final states. This summation can be approximated to an integral and the cross section for the inclusive production process can be written as [59]

$$\sigma = \int \int \left( \frac{d^2\sigma}{dm dt} \right) dm dt \quad (3)$$

$$\frac{d^2\sigma}{dm dt} = \frac{2\pi^{\delta/2}}{\Gamma(\delta/2)} \frac{\bar{M}_{Pl}^2}{M_D^{2+\delta}} m^{\delta-1} \frac{d\sigma_m}{dt} \quad (4)$$

where  $\frac{d\sigma_m}{dt}$  is the cross section for producing a single KK graviton state of mass  $m$ . The differential cross section  $\frac{d\sigma_m}{dt}$  can be obtained in conventional way from the scattering amplitude. Since the masses of KK states are integrated, total cross section in Eq. (3) depends on two model parameters  $M_D$  and  $\delta$ .

In the RS model case, the spectrum of KK graviton masses is given by [61]

$$m_n = x_n k e^{-kr_c\pi} = x_n \beta \Lambda_\pi, \quad \beta = k/\bar{M}_{Pl} \quad (5)$$

where  $x_n$  are the roots of the Bessel function  $J_1$ , i.e.,  $J_1(x_n) = 0$ . We can deduce from this formula that mass splitting between consecutive KK graviton states is considerably large,

$\sim \mathcal{O}(TeV)$ . Hence it is assumed that only the first KK graviton state can be observed. We will represent the mass of this first KK graviton state by  $m_G$ . Masses of other KK states are proportional to  $m_G$ :  $m_n = \frac{x_n}{x_1} m_G$ . In the RS model we have two independent model parameters. We prefer to choose  $m_G$  and  $\beta$  as independent parameters.

The process  $\gamma q \rightarrow Gq$  is represented by the Feynman diagrams in Fig.2. We do not give the Feynman rules for KK gravitons. One can find the Feynman rules in Refs. [59, 60]. Analytical expressions for the scattering amplitude are given in the Appendix. As we have mentioned in the introduction we consider all possible initial quark flavors. Thus, in order to obtain the total cross section for the process  $pp \rightarrow p\gamma p \rightarrow pGqX$  we integrate the subprocess cross sections over the photon and quark distributions and sum all contributions from different subprocesses:

$$\sigma(pp \rightarrow p\gamma p \rightarrow pGqX) = \sum_q \int_{\xi_{min}}^{\xi_{max}} dx_1 \int_0^1 dx_2 \left( \frac{dN_\gamma}{dx_1} \right) \left( \frac{dN_q}{dx_2} \right) \sigma(\gamma q \rightarrow Gq) \quad (6)$$

Here,  $x_1$  represents the energy ratio between the equivalent photon and incoming proton and  $x_2$  is the fraction of the proton's momentum carried by the struck quark.  $\frac{dN_\gamma}{dx_1}$  and  $\frac{dN_q}{dx_2}$  are the equivalent photon and quark distribution functions. The analytical expression for  $\frac{dN_\gamma}{dx_1}$  can be found in the literature, for example in [9–12] or [30].  $\frac{dN_q}{dx_2}$  can be evaluated numerically. In this paper we have used parton distribution functions of Martin *et al.* [62].

### III. NUMERICAL RESULTS

During numerical calculations we assume the existence of VFD proposed by Refs. [22, 30, 63, 64]. In Refs. [22, 63], it was proposed to locate VFD at 220 m and 420 m distances away from the ATLAS interaction point. These detectors can detect forward protons within the acceptance region  $0.0015 < \xi < 0.15$ . Here,  $\xi \equiv (|\vec{p}| - |\vec{p}'|)/|\vec{p}|$  where  $\vec{p}$  represents the initial proton's momentum and  $\vec{p}'$  represents forward proton's momentum after scattering. According to another scenario VFD can detect forward protons within  $0.0015 < \xi < 0.5$  [30, 64]. This scenario is based on VFD located at 420 m distance from the CMS interaction point and TOTEM detectors at 147 m and 220 m.

For all numerical results presented in this paper, the center of mass energy of the proton-proton system is taken to be  $\sqrt{s} = 14$  TeV and the virtuality of the DIS is taken to be  $Q^2 = (5M_Z)^2 \approx (456 GeV)^2$ . Here,  $M_Z$  is the mass of the Z boson and it represents only

a scale which is roughly at the order of Standard Model energies. This virtuality value is reasonable since the average value for the square of the momentum transferred to the proton is approximately at that order. Moreover, at high energies parton distribution functions do not depend significantly on virtuality. Thus, it is reasonable to use a fix virtuality value for the DIS.

In Fig.3 and Fig.4 we present ADD model cross section of the process  $pp \rightarrow p\gamma p \rightarrow pGqX$  as a function of the fundamental scale  $M_D$  for VFD acceptances of  $0.0015 < \xi < 0.5$  and  $0.0015 < \xi < 0.15$  respectively. We consider the cases in which the number of extra spatial dimensions are  $\delta = 3, 4, 5, 6$ . We see from these figures that cross section decreases with increasing  $\delta$ . Moreover, cross sections for different number of extra dimensions significantly deviate from each other for large  $M_D$  values. These behaviors are obvious from differential cross section formula in Eq. (4). As we have discussed in the previous section, ADD graviton final states consist of huge number of KK states arranged densely with increasing mass. This sequence of states is sometimes called a KK tower. A KK tower is not detected directly in the detectors. Instead, their presence is inferred from missing energy signal. Missing signal for a KK tower exhibits a peculiarity which is very different compared with any other new physics processes [59]. This peculiar behavior for a KK tower can be observed from the transverse momentum distribution. Hence, in Fig.5-Fig.8 we present missing  $p_T$  ( $p_T$  of the KK tower) dependence of the cross section of the process  $pp \rightarrow p\gamma p \rightarrow pGqX$  for various number of extra dimensions  $\delta$ . In these figures VFD acceptance is taken to be  $0.0015 < \xi < 0.5$  and  $M_D=5$  TeV.  $p_T$  distributions for  $0.0015 < \xi < 0.15$  case exhibit similar behaviors.

In the RS model, we aim to observe first KK graviton state with mass  $m_G$ . Similar to techniques used to detect a massive particle such as  $W, Z$  boson or top quark, an RS graviton can be detected from its decay products. Angular distribution of the RS graviton for the process  $pp \rightarrow p\gamma p \rightarrow pGqX$  is given in Fig.9. We consider VFD acceptance of  $0.0015 < \xi < 0.5$  but we expect a similar behavior for  $0.0015 < \xi < 0.15$  case. In the figure, we show both the the cross section including the sum of all contributions from subprocesses in (1) and cross sections including individual contributions from each subprocess.

We have obtained 95% confidence level (CL) bounds on the model parameters of the ADD and RS models. Since the Standard Model contribution to the process is absent it is appropriate to employ a statistical analysis using a Poisson distribution. In the ADD model case, the expected number of events is calculated from the formula:  $N = S \times E \times \sigma(pp \rightarrow$

$p\gamma p \rightarrow pGqX) \times L_{int}$ . In this formula,  $S$  represents the survival probability factor,  $E$  represents the jet reconstruction efficiency and  $L_{int}$  represents the integrated luminosity. We take into account a survival probability factor of  $S = 0.7$  and jet reconstruction efficiency of  $E = 0.6$ . We also place a pseudorapidity cut of  $|\eta| < 2.5$  for final quarks and antiquarks from subprocesses in (1). The 95% CL bounds on the fundamental scale are given in Tables I and II for various values of  $L_{int}$  and  $\delta$ . In the RS model, bounds are calculated in the plane of  $\beta$  versus  $m_G$ . Since an RS graviton can be detected from its decay products, the expected number of events is given by  $N = S \times E \times \sigma(pp \rightarrow p\gamma p \rightarrow pGqX) \times L_{int} \times BR$ , where  $BR$  represents the branching ratio for the graviton. The limits have been calculated by considering two different branching ratio values. In the first case, we have taken account of  $G \rightarrow \gamma\gamma, e\bar{e}, \mu\bar{\mu}$  decay channels of the RS graviton with a total branching ratio of 8% [65]. In the second case, in addition to the first decay channels we have taken account of quark-antiquark and gluon-gluon decays of the graviton, i.e.,  $G \rightarrow \gamma\gamma, e\bar{e}, \mu\bar{\mu}, q\bar{q}, gg$ . Branching ratio is quite large for the second case. It is approximately 68% [65]. In Fig.10 and Fig.11 we present the excluded regions in the  $\beta$  versus  $m_G$  parameter plane for the above branching ratio values. We see from these figures that the limits for  $BR = 68\%$  case are approximately 150% better than the case for  $BR = 8\%$ .

## Acknowledgments

This work has been supported by the Scientific and Technological Research Council of Turkey (TÜBİTAK) in the framework of the project no: 112T085.

## Appendix: Analytical expressions for the scattering amplitude

In the ADD model of extra dimensions the polarization summed amplitude square for the subprocess  $\gamma q \rightarrow Gq$  is given by

$$|M|^2 = |M_1 + M_2 + M_3 + M_4|^2 \quad (\text{A.1})$$

$$|M_1|^2 = -\frac{(gg_e)^2 [40(m^4 - (s - t + u)m^2 + su)]}{4\bar{M}_{Pl}^2 3m^2} \quad (\text{A.2})$$

$$|M_2|^2 = \frac{(qg_e)^2}{3t^2m^4\bar{M}_{Pl}^2} [-6m^{10} + 12tm^8 + 6((s+u)^2 - 2t^2)m^6 - 2t(6s^2 + ts - 6t^2 + 6u^2 + tu)m^4 + 2t^2(4s^2 + (t-4u)s - (3t-4u)(t+u))m^2 - 2t^3(s^2 + u^2)] \quad (\text{A.3})$$

$$M_1^\dagger M_2 + M_2^\dagger M_1 = \frac{(qg_e)^2}{2t\bar{M}_{Pl}^2} \frac{[20(-2m^6 + (2s+t+2u)m^4 - 2t(s+u)m^2 + t^3 + 2stu)]}{3m^2} \quad (\text{A.4})$$

$$|M_3|^2 = -\frac{(qg_e)^2}{48s^2m^4\bar{M}_{Pl}^2} [4s(2m^8 - (5s+t-4u)m^6 + 2(2s^2 - 4us + (t+u)(t+2u))m^4 - (s+3t-2u)(-s+t+u)^2m^2 + 2st(-s+t+u)^2)] \quad (\text{A.5})$$

$$M_1^\dagger M_3 + M_3^\dagger M_1 = -\frac{(qg_e)^2}{24sm^4\bar{M}_{Pl}^2} [32m^8 + (-60s + 4t - 68u)m^6 + 8(3s^2 + (t+7u)s + (t+u)(2t+5u))m^4 + 4(s^3 - 3(t-u)s^2 + 3(t-5u)(t+u)s - (t+u)^3)m^2 - 16s(s-t-u)u(t+u)] \quad (\text{A.6})$$

$$M_2^\dagger M_3 + M_3^\dagger M_2 = -\frac{(qg_e)^2}{12tsm^4\bar{M}_{Pl}^2} [2((13s+3t-3u)m^8 - 2(12s^2 + 9ts - 4t^2 + 4(s+t)u)m^6 + (12s^3 + (6t+9u)s^2 + t(25t+13u)s - (t-u)(13t^2 + 24ut + 3u^2))m^4 - (s^4 + (u-6t)s^3 + (11t^2 + 16ut - u^2)s^2 + (8t^3 + 15ut^2 - 2u^2t - u^3)s - 2t(t-u)(t+u)(t+6u))m^2 - 2t(s-t-u)(u^3 - t^2u + s^2(2t+3u)))] \quad (\text{A.7})$$

$$|M_4|^2 = -\frac{(qg_e)^2}{48u^2m^4\bar{M}_{Pl}^2} [4u(2m^8 + (4s-t-5u)m^6 + 2(2s^2 + 3ts - 4us + t^2 + 2u^2)m^4 + (2s-3t-u)(s+t-u)^2m^2 + 2t(s+t-u)^2u)] \quad (\text{A.8})$$

$$M_1^\dagger M_4 + M_4^\dagger M_1 = -\frac{(qg_e)^2}{24um^4\bar{M}_{Pl}^2} [4(8m^8 + (-17s + t - 15u)m^6 + 2(5s^2 + 7(t + u)s + 2t^2 + 3u^2 + tu)m^4 + (-(s + t)^3 - 3(5s - t)u(s + t) + u^3 + 3(s - t)u^2)m^2 + 4s(s + t)(s + t - u)u)] \quad (\text{A.9})$$

$$M_2^\dagger M_4 + M_4^\dagger M_2 = -\frac{(qg_e)^2}{12tum^4\bar{M}_{Pl}^2} [2((-3s + 3t + 13u)m^8 - 2(-4t^2 + 9ut + 12u^2 + 4s(t + u))m^6 + (3s^3 + 21ts^2 - 11t^2s - 13t^3 + 12u^3 + 3(3s + 2t)u^2 + t(13s + 25t)u)m^4 - (u^4 + (s - 6t)u^3 - (s^2 - 16ts - 11t^2)u^2 - (s^3 + 2ts^2 - 15t^2s - 8t^3)u + 2(s - t)t(s + t)(6s + t))m^2 + 2t(s + t - u)(s^3 - t^2s + 3u^2s + 2tu^2))] \quad (\text{A.10})$$

$$M_3^\dagger M_4 + M_4^\dagger M_3 = \frac{(qg_e)^2}{48sum^4\bar{M}_{Pl}^2} [4(8tm^8 + (s^2 - 15ts - 2us - 30t^2 + u^2 - 15tu)m^6 + (-6s^3 + 6us^2 + (26t^2 + 72ut + 6u^2)s - 12t^3 - 6u^3 + 26t^2u)m^4 + (3s^4 + (13t + 8u)s^3 - (13t^2 + 13tu + 22u^2)s^2 - (13t^3 + 18ut^2 + 13u^2t - 8u^3)s + (2t - 3u)(t - u)(5t + u))m^2 + 2(s - t - u)(s + t - u)(s^3 - us^2 - (t + u)^2s + u^3 - t^2u))] \quad (\text{A.11})$$

where  $M_1$ ,  $M_2$ ,  $M_3$  and  $M_4$  are the amplitudes of the Feynman diagrams in Fig.2,  $s$ ,  $t$  and  $u$  are Mandelstam parameters,  $m$  is the mass of the individual KK graviton,  $g_e = \sqrt{4\pi\alpha}$ ,  $q = -\frac{1}{3}$  for d,s and b quarks and  $q = +\frac{2}{3}$  for u and c quarks. During amplitude calculations we neglect the mass of quarks. This is a good approximation at the LHC energies.

The amplitude square in the RS model can be obtained by the following replacement:  
 $\bar{M}_{Pl} \rightarrow \sqrt{2} \Lambda_\pi$

---

[1] X. Rouby, Ph.D. thesis, Universite Catholique de Louvain [CERN-THESIS-2009-216 and CMS-TS-2009-004]

- [2] N. Schul, Ph.D. thesis, Universite Catholique de Louvain [CERN-THESIS-2011-271 and CMS-TS-2011-030].
- [3] S. Atağ, S. C. İnan and İ. Şahin, Phys. Rev. D **80**, 075009 (2009); arXiv:0904.2687 [hep-ph].
- [4] S. Atağ, S. C. İnan and İ. Şahin, JHEP **09**, 042 (2010); arXiv:1005.4792 [hep-ph].
- [5] H. Sun, Eur. Phys. J. C **74**, 2977 (2014) [arXiv:1406.3897 [hep-ph]].
- [6] V. P. Goncalves and W. K. Sauter, Phys. Rev. D **82**, 056009 (2010) [arXiv:1007.5487 [hep-ph]].
- [7] S. C. Inan and A. A. Billur, Phys. Rev. D **84**, 095002 (2011).
- [8] S. C. Inan, Chin. Phys. Lett. **29**, 031301 (2012).
- [9] İ. Şahin *et al.*, Phys. Rev. D **88**, 095016 (2013) [arXiv:1304.5737 [hep-ph]].
- [10] V. M. Budnev, I. F. Ginzburg, G. V. Meledin and V. G. Serbo, Phys. Rep. **15**, 181 (1975).
- [11] G. Baur *et al.*, Phys. Rep. **364**, 359 (2002).
- [12] K. Piotrkowski, Phys. Rev. D **63**, 071502 (2001) [hep-ex/0009065].
- [13] M. Albrow *et al.* (CMS Collaboration), JINST **4**, P10001 (2009) [arXiv:0811.0120 [hep-ex]].
- [14] A. Abulencia *et al.* (CDF Collaboration), Phys. Rev. Lett. **98**, 112001 (2007); arXiv:hep-ex/0611040.
- [15] T. Aaltonen *et al.* (CDF Collaboration), Phys. Rev. Lett. **102**, 222002 (2009) [arXiv:0902.2816 [hep-ex]].
- [16] T. Aaltonen *et al.* (CDF Collaboration), Phys. Rev. Lett. **108**, 081801 (2012) [arXiv:1112.0858 [hep-ex]].
- [17] T. Aaltonen *et al.* (CDF Collaboration), Phys. Rev. D **77**, 052004 (2008) [arXiv:0712.0604 [hep-ex]].
- [18] T. Aaltonen *et al.* (CDF Collaboration), Phys. Rev. Lett. **102**, 242001 (2009) [arXiv:0902.1271 [hep-ex]].
- [19] S. Chatrchyan *et al.* (CMS Collaboration), JHEP **1201**, 052 (2012) [arXiv:1111.5536 [hep-ex]].
- [20] S. Chatrchyan *et al.* (CMS Collaboration), JHEP **1211**, 080 (2012) [arXiv:1209.1666 [hep-ex]].
- [21] S. Chatrchyan *et al.* (CMS Collaboration), JHEP **1307**, 116 (2013) [arXiv:1305.5596 [hep-ex]].
- [22] M. G. Albrow *et al.* (FP420 R and D Collaboration), JINST **4**, T10001 (2009) [arXiv:0806.0302 [hep-ex]].
- [23] M. G. Albrow, T. D. Coughlin and J. R. Forshaw, Prog. Part. Nucl. Phys. **65**, 149 (2010) [arXiv:1006.1289 [hep-ph]].
- [24] I. F. Ginzburg and A. Schiller, Phys. Rev. D **57**, 6599 (1998) [hep-ph/9802310].

- [25] I. F. Ginzburg and A. Schiller, Phys. Rev. D **60**, 075016 (1999) [hep-ph/9903314].
- [26] S. M. Lietti, A. A. Natale, C. G. Roldao and R. Rosenfeld, Phys. Lett. B **497**, 243 (2001); arXiv:hep-ph/0009289.
- [27] V.A. Khoze, A.D. Martin and M.G. Ryskin, Eur. Phys. J. C **23**, 311 (2002); arXiv:hep-ph/0111078.
- [28] N. Schul and K. Piotrkowski, Nucl. Phys. B, Proc. Suppl., **179**, 289 (2008); arXiv:0806.1097 [hep-ph].
- [29] T. Pierzchala and K. Piotrkowski, Nucl. Phys. Proc. Suppl. **179-180**, 257 (2008); arXiv:0807.1121 [hep-ph].
- [30] O. Kepka and C. Royon, Phys. Rev. D **78**, 073005 (2008); arXiv:0808.0322 [hep-ph].
- [31] İ. Şahin and S. C. İnan, JHEP **09**, 069 (2009); arXiv:0907.3290 [hep-ph].
- [32] T. Dougall and S. D. Wick, Eur. Phys. J. A **39**, 213 (2009) [arXiv:0706.1042 [hep-ph]].
- [33] M. Chaichian, P. Hoyer, K. Huitu, V. A. Khoze and A. D. Pilkington, JHEP **0905**, 011 (2009) [arXiv:0901.3746 [hep-ph]].
- [34] J. de Favereau de Jeneret, V. Lemaitre, Y. Liu, S. Oryn, T. Pierzchala, K. Piotrkowski, X. Rouby, N. Schul and M. Vander Donckt, arXiv:0908.2020 [hep-ph].
- [35] E. Chapon, C. Royon and O. Kepka, Phys. Rev. D **81**, 074003 (2010); arXiv:0912.5161 [hep-ph].
- [36] K. Piotrkowski and N. Schul, AIP Conf. Proc. **1200**, 434 (2010) [arXiv:0910.0202 [hep-ph]].
- [37] S. C. İnan, Phys. Rev. D **81**, 115002 (2010); arXiv:1005.3432 [hep-ph].
- [38] S. Atağ and A. A. Billur, JHEP **11**, 060 (2010); arXiv:1005.2841 [hep-ph].
- [39] İ. Şahin, and A. A. Billur, Phys. Rev. D **83**, 035011 (2011); arXiv:1101.4998 [hep-ph].
- [40] İ. Şahin, and M. Koksal, JHEP **03**, 100 (2011); arXiv:1010.3434 [hep-ph].
- [41] R. S. Gupta, Phys. Rev. D **85**, 014006 (2012) [arXiv:1111.3354 [hep-ph]].
- [42] İ. Şahin, Phys. Rev. D **85**, 033002 (2012) [arXiv:1201.4364 [hep-ph]].
- [43] L. N. Epele, H. Fanchiotti, C. A. G. Canal, V. A. Mitsou and V. Vento, Eur. Phys. J. Plus **127**, 60 (2012) [arXiv:1205.6120 [hep-ph]].
- [44] B. Şahin and A. A. Billur, Phys. Rev. D **86**, 074026 (2012) [arXiv:1210.3235 [hep-ph]].
- [45] İ. Şahin and B. Şahin, Phys. Rev. D **86**, 115001 (2012) [arXiv:1211.3100 [hep-ph]].
- [46] A. A. Billur, Europhys. Lett. **101**, 21001 (2013).
- [47] A. Senol, Phys. Rev. D **87**, 073003 (2013) [arXiv:1301.6914 [hep-ph]].

- [48] M. Koksal and S. C. Inan, Adv. High Energy Phys. **2014**, 935840, (2014) [arXiv:1305.7096 [hep-ph]].
- [49] H. Sun and C. X. Yue, Eur. Phys. J. C **74**, 2823 (2014) [arXiv:1401.0250 [hep-ph]].
- [50] H. Sun, Nucl. Phys. B **886**, 691 (2014) [arXiv:1402.1817 [hep-ph]].
- [51] A. Senol, A. T. Tasci, I. T. Cakir and O. Cakir, arXiv:1405.6050 [hep-ph].
- [52] M. Koksal and S. C. Inan, Adv. High Energy Phys. **2014**, 315826 (2014) [arXiv:1403.2760 [hep-ph]].
- [53] H. Sun, arXiv:1407.5356 [hep-ph].
- [54] H. Sun, Y. J. Zhou and H. S. Hou, arXiv:1408.1218 [hep-ph].
- [55] N. Arkani-Hamed, S. Dimopoulos and G. R. Dvali, Phys. Lett. B **429**, 263 (1998) [hep-ph/9803315].
- [56] N. Arkani-Hamed, S. Dimopoulos and G. R. Dvali, Phys. Rev. D **59**, 086004 (1999) [hep-ph/9807344].
- [57] I. Antoniadis, N. Arkani-Hamed, S. Dimopoulos and G. R. Dvali, Phys. Lett. B **436**, 257 (1998) [hep-ph/9804398].
- [58] L. Randall and R. Sundrum, Phys. Rev. Lett. **83**, 3370 (1999) [hep-ph/9905221].
- [59] G. F. Giudice, R. Rattazzi and J. D. Wells, Nucl. Phys. B **544**, 3 (1999) [hep-ph/9811291].
- [60] T. Han, J. D. Lykken and R. -J. Zhang, Phys. Rev. D **59**, 105006 (1999) [hep-ph/9811350].
- [61] H. Davoudiasl, J. L. Hewett and T. G. Rizzo, Phys. Rev. Lett. **84**, 2080 (2000) [hep-ph/9909255].
- [62] A. D. Martin, W. J. Stirling, R. S. Thorne and G. Watt, Eur. Phys. J. C **63**, 189 (2009) [arXiv:0901.0002 [hep-ph]].
- [63] C. Royon (RP220 Collaboration), arXiv:0706.1796.
- [64] V. Avati and K. Osterberg, Report No. CERN-TOTEM-NOTE-2005-002, 2006.
- [65] B. C. Allanach, K. Odagiri, M. J. Palmer, M. A. Parker, A. Sabetfakhri and B. R. Webber, JHEP **0212**, 039 (2002) [hep-ph/0211205].

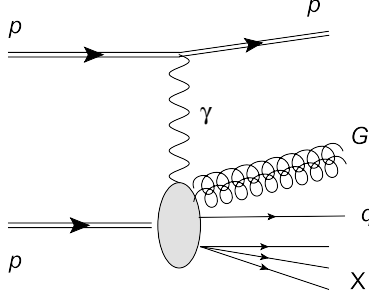


FIG. 1: The photoproduction process  $pp \rightarrow p\gamma p \rightarrow pGqX$ .

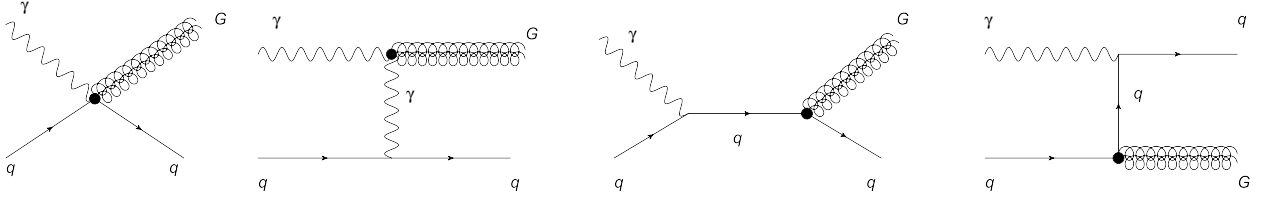


FIG. 2: Tree-level Feynman diagrams for the subprocess  $\gamma q \rightarrow Gq$  ( $q = u, d, c, s, b, \bar{u}, \bar{d}, \bar{c}, \bar{s}, \bar{b}$ ).

TABLE II: The 95% C.L. bounds on  $M_D$  for various integrated LHC luminosities and forward detector acceptance of  $0.0015 < \xi < 0.15$ . Bounds are given in units of GeV.

Luminosity	$\delta = 3$	$\delta = 4$	$\delta = 5$	$\delta = 6$
$30fb^{-1}$	4560	4112	3552	3356
$50fb^{-1}$	5028	4224	3804	3608
$100fb^{-1}$	5784	4748	4224	3916
$200fb^{-1}$	6636	5336	4692	4280

TABLE I: The 95% C.L. bounds on  $M_D$  for various integrated LHC luminosities and forward detector acceptance of  $0.0015 < \xi < 0.5$ . Bounds are given in units of GeV.

Luminosity	$\delta = 3$	$\delta = 4$	$\delta = 5$	$\delta = 6$
$30fb^{-1}$	5314	4714	4486	4400
$50fb^{-1}$	5886	5143	4829	4686
$100fb^{-1}$	6743	5771	5343	5114
$200fb^{-1}$	7771	6514	5886	5571

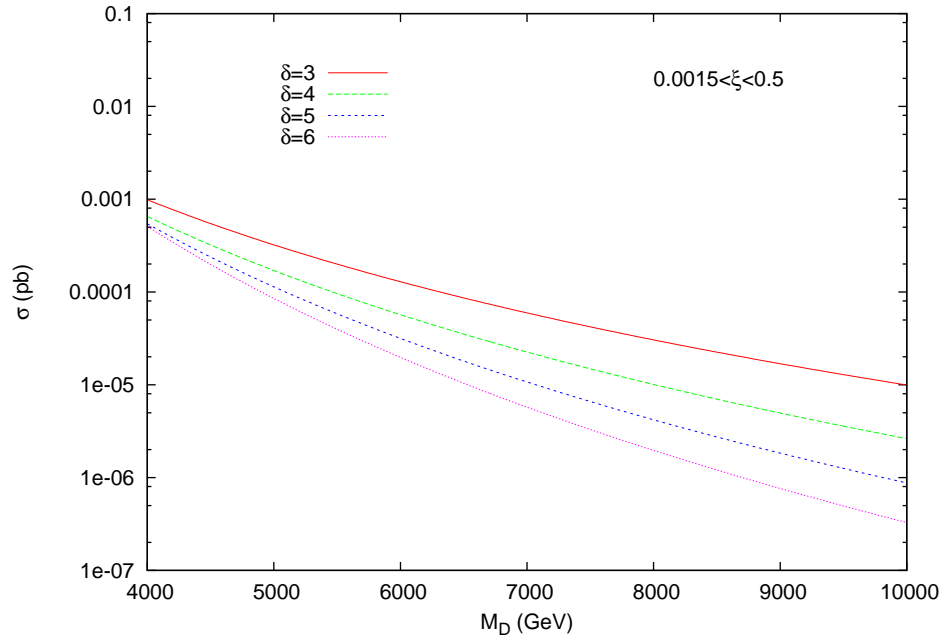


FIG. 3: The total cross section of the process  $pp \rightarrow p\gamma p \rightarrow pGqX$  as a function of the fundamental scale  $M_D$  for various number of extra dimensions  $\delta$ . The forward detector acceptance is chosen to be  $0.0015 < \xi < 0.5$ .

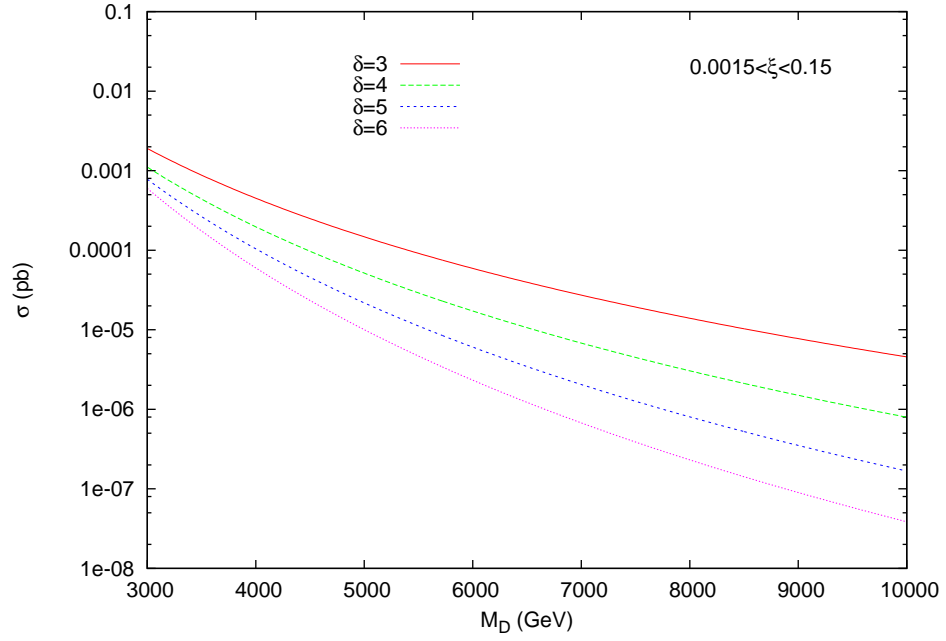


FIG. 4: The total cross section of the process  $pp \rightarrow p\gamma p \rightarrow pGqX$  as a function of the fundamental scale  $M_D$  for various number of extra dimensions  $\delta$ . The forward detector acceptance is chosen to be  $0.0015 < \xi < 0.15$ .

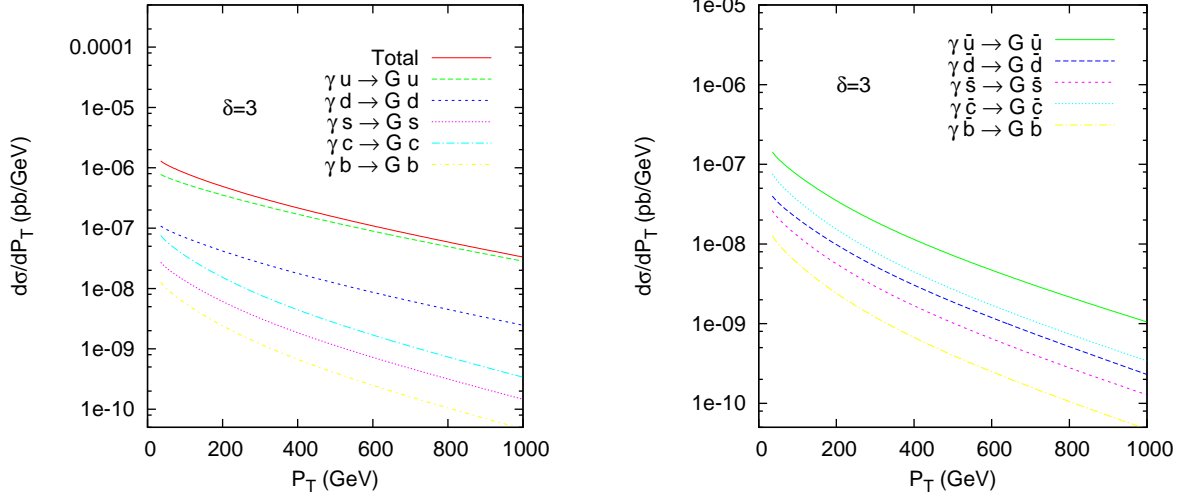


FIG. 5: The differential cross section of the process  $pp \rightarrow p\gamma p \rightarrow pGqX$  as a function of the transverse momentum of the KK tower. The number of extra dimensions is chosen to be  $\delta = 3$  and  $M_D = 5$  TeV. In the left panel we present total cross section (solid line) which represents the sum of all contributions from subprocesses in (1) and cross sections including individual contributions from each subprocess with quarks. In the right panel we present similar plots but for subprocesses with antiquarks.

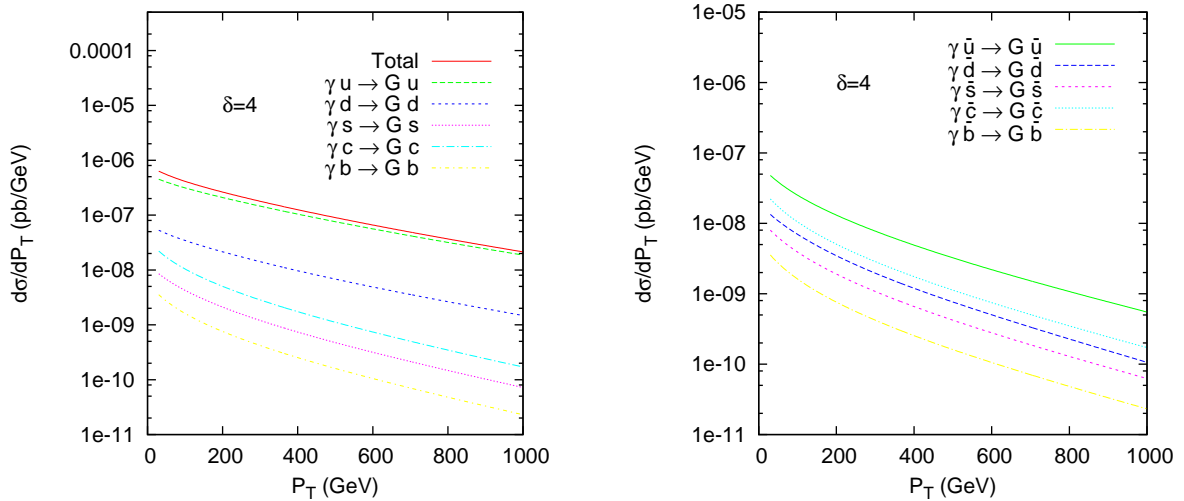


FIG. 6: The same as figure 5 but for  $\delta = 4$ .

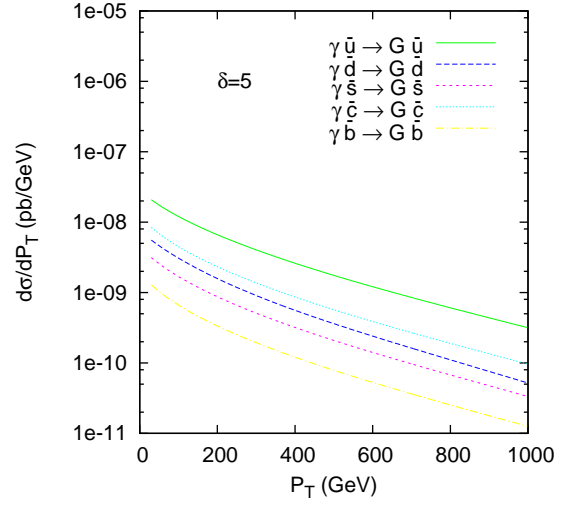
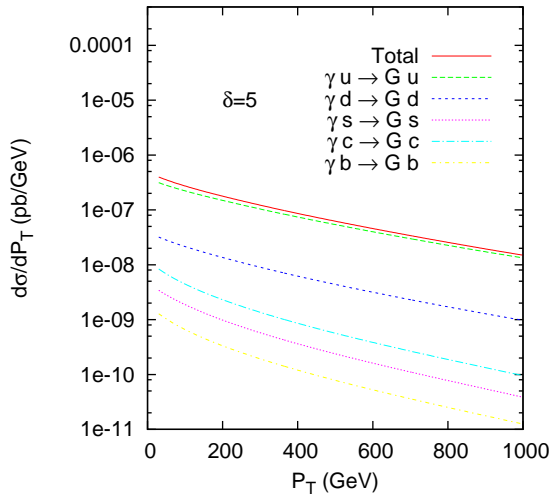


FIG. 7: The same as figure 5 but for  $\delta = 5$ .

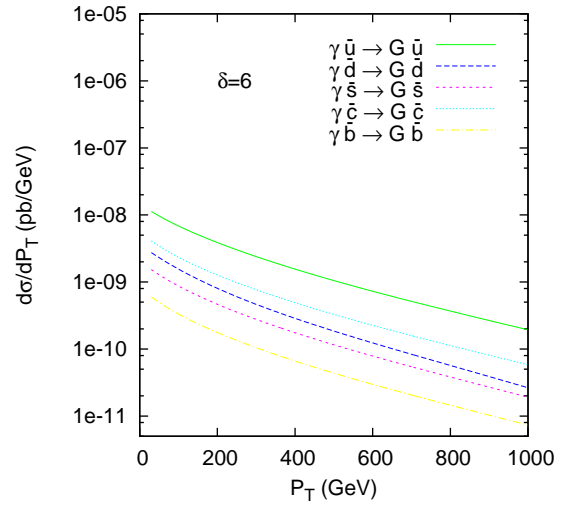
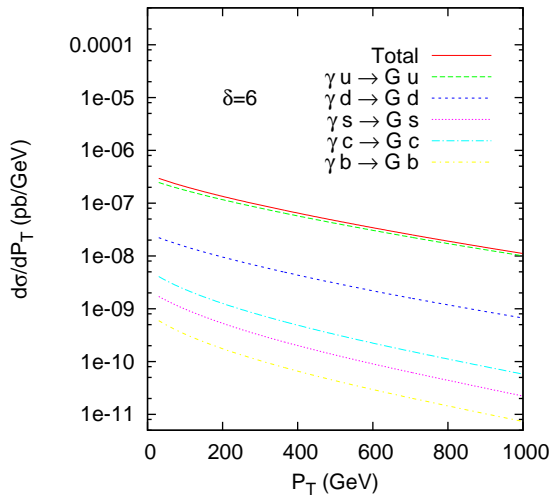


FIG. 8: The same as figure 5 but for  $\delta = 6$ .

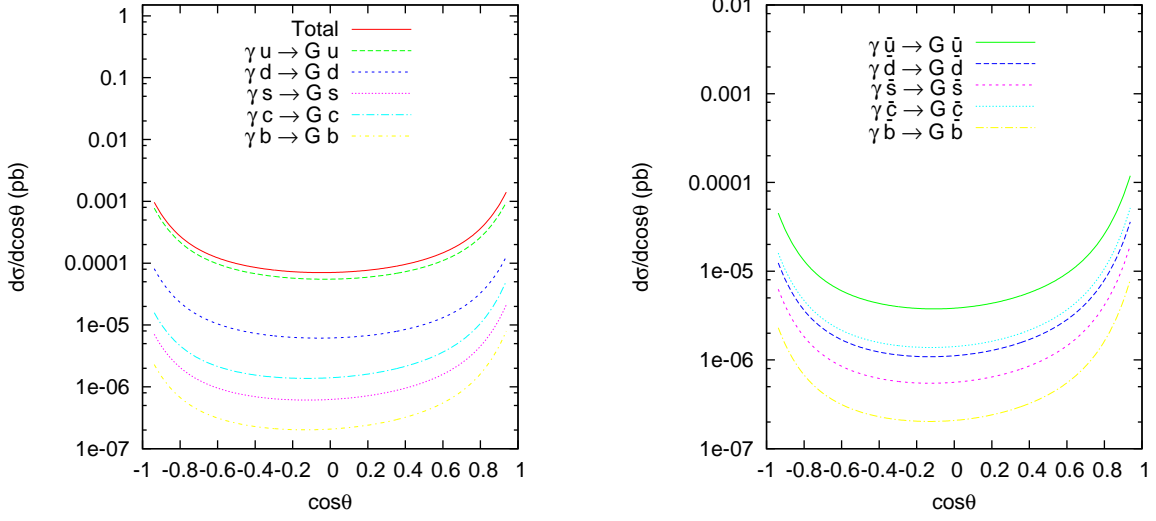


FIG. 9: The angular distribution of the graviton in the center-of-momentum frame of the proton-proton system.  $\theta$  is the angle between the outgoing graviton and the incoming photon emitting intact proton. RS model parameters are chosen to be  $\beta = 0.05$  and  $m_G = 1$  TeV. In the left panel we present total cross section (solid line) which represents the sum of all contributions from subprocesses in (1) and cross sections including individual contributions from each subprocess with quarks. In the right panel we present similar plots but for subprocesses with antiquarks.

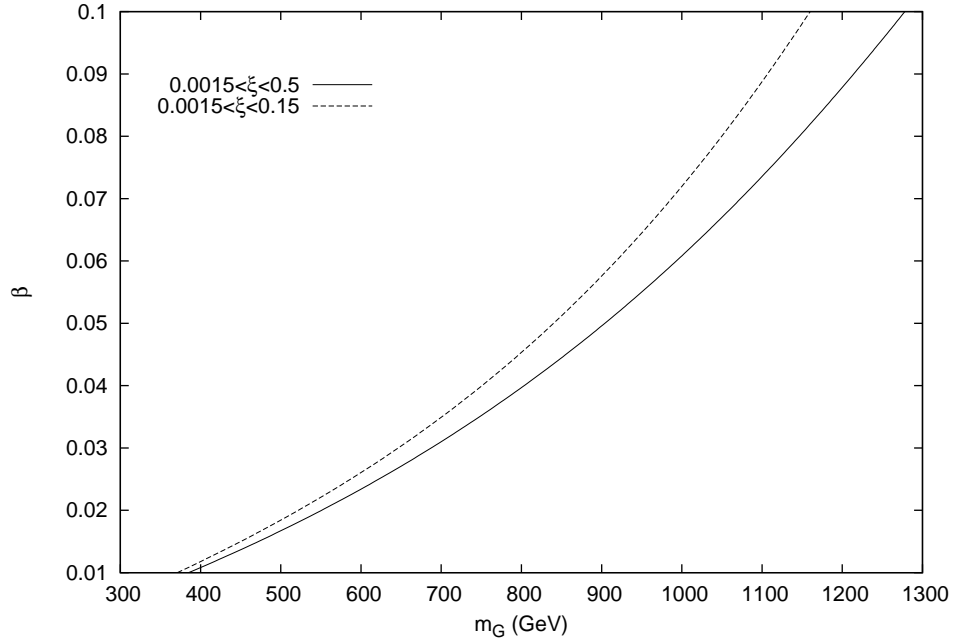


FIG. 10: The 95% C.L. limits in the RS parameter space for an integrated luminosity of  $200 \text{ fb}^{-1}$ . The excluded regions are defined by the area above the curves.  $G \rightarrow \gamma\gamma, e\bar{e}, \mu\bar{\mu}$  decay channels with a total branching ratio of 8% is considered.

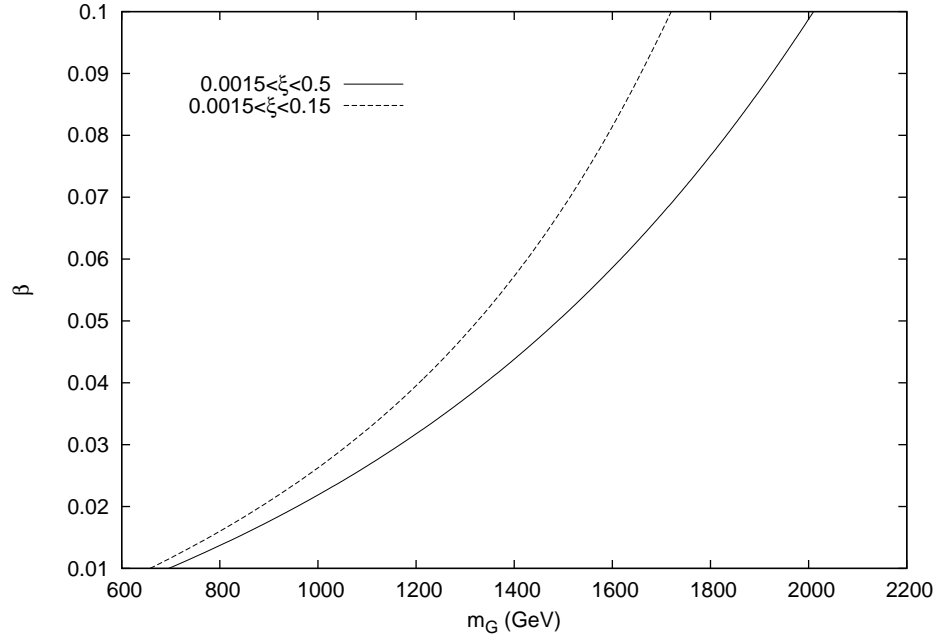


FIG. 11: The 95% C.L. limits in the RS parameter space for an integrated luminosity of  $200 \text{ fb}^{-1}$ . The excluded regions are defined by the area above the curves.  $G \rightarrow \gamma\gamma, e\bar{e}, \mu\bar{\mu}, q\bar{q}, gg$  decay channels with a total branching ratio of 68% is considered.